

Deep Learning-Based Modulation Detection for NOMA Systems

Wenwu Xie¹, Jian Xiao¹, Jinxia Yang¹, Ji Wang^{2*}, Xin Peng¹, Chao Yu¹, and Peng Zhu¹

¹School of Information Science and Engineering, Hunan Institute of Science and Technology
Hunan, 414000, China

[e-mail: gavinxie@hnist.edu.cn, jianchongren@sina.com]

²College of Physical Science and Technology, Central China Normal University
Hubei, 430000, China

[e-mail: jiwang@ccnu.edu.cn]

*Corresponding author: Ji Wang

*Received October 18, 2020; revised December 10, 2020; accepted January 5, 2021;
published February 28, 2021*

Abstract

Since the signal with strong power need be demodulated first for successive interference cancellation (SIC) receiver in non-orthogonal multiple access (NOMA) systems, the base station (BS) need inform the near user terminal (UT), which has allocated higher power, of the far UT's modulation mode. To avoid unnecessary signaling overhead of control channel, a blind detection algorithm of NOMA signal modulation mode is designed in this paper. Taking the joint constellation density diagrams of NOMA signal as the detection features, the deep residual network is built for classification, so as to detect the modulation mode of NOMA signal. In view of the fact that the joint constellation diagrams are easily polluted by high intensity noise and lose their real distribution pattern, the wavelet denoising method is adopted to improve the quality of constellations. The simulation results represent that the proposed algorithm can achieve satisfactory detection accuracy in NOMA systems. In addition, the factors affecting the recognition performance are also verified and analyzed.

Keywords: Modulation Detection, NOMA, Wavelet Denoising, Residual Network

This work was supported in part by the Natural Science Foundation of China under Grant 61772195, in part by the Natural Science Foundation of Hunan Province, China under Grant 2018JJ2154 and 2020JJ4341, in part by the Science and Technology Program of Hunan Province under Grant 2016TP1021, in part by the Outstanding Youth Project of Hunan Provincial Education Department under Grant 18B353, 19K037, 20B267 and 20B269, in part by the Emergency Communication Engineering Technology Research Center of Hunan Province under Grant 2018TP2022, and the Hunan Institute of Science and Technology for Postgraduate under Grant YCK2020A38.

1. Introduction

The communication of massive Internet of Things (IoT) requires wireless networks with higher spectral efficiency, lower latency and larger transmission capacity. In the face of the above requirements for higher communication quality, a new multiple access multiplexing method, namely non-orthogonal multiple access (NOMA) was proposed [1]. The research object of this paper is the power domain NOMA, which is the NOMA protocol commonly used at present [2]. In NOMA systems, the base station (BS) exploits the power domain by allocating the same communication resource but different power level to multiple-user (MU) for downlink transmissions. In the downlink NOMA, user terminals (UTs) with poor channel conditions will be allocated larger power to compensate its low channel gain, which are called far UT, and near UT with better channel conditions will be allocated lower power, which is closer the BS than the far UT. Although interference information is introduced in NOMA system, successive interference cancellation (SIC) technology can be utilized at user terminal for removing it [2, 3], and thus higher spectral efficiency can be achieved. From the perspective of modulation scheme, the signals transmitted by the BS contain multiple modulation schemes when each user uses a different modulation scheme to encode the signal. Due to the protocol of NOMA technology, SIC receiver needs to first demodulate the signal desired to far UT, which requires the knowledge of modulation mode for that signal. The general solution is to inform the UT through signaling, which can lead to a higher transmission delay in massive IoT scenarios containing enormous devices. Therefore, the implementation of blind modulation detection at near user can reduce signaling overhead of control channel for SIC demodulation and further improve the quality of service in NOMA systems.

The NOMA signal is essentially a time-frequency overlapped modulation signal. Some research has been done for the modulation recognition of overlapped signals in orthogonal multiple access (OMA) systems, such as using cyclo-stationary theory to extract the feature of signal component [4]. However, The NOMA signal is completely overlapped in time-frequency domain, in which case, many existing single channel signal modulation recognition algorithm is often no longer applicable without any prior knowledge information. In [5], the maximum likelihood algorithm is used to implement the modulation detection in NOMA systems, which is extended by the ML algorithm in OMA systems [6]. However, the ML algorithm often has a high computational complexity. The work of [7] studied the detection of interference modulation order in downlink NOMA systems, which extracts feature vector based on Anderson-Darling test, and then classify by logistic regression model, but channel equalization is required for extracting effective feature before blind detection.

Artificial intelligence technology provides new ideas for designing the next generation of wireless communication systems, which has become a research hotspot in the industry [8, 9]. A deep learning (DL)-aided NOMA system is designed by using long short-term memory network, which can detect the channel characteristics intelligently [10]. In [11], the deep neural network is used to construct the precoder and SIC decoder in MIMO-NOMA system. Both precoding and SIC decoding of the MIMO-NOMA system are jointly optimized, which enables the received signal to be accurately decoded. The application of DL into signal recognition, especially on modulation classification, has attracted most research interests due to its strong feature learning ability [12-14]. The baseband signal is acted as the input of the neural network, and the classical deep network architecture is used for modulation detection in [12], whose results show that further advances for DL-based modulation detection likely come from improved training algorithm and novel network design. The key to the improvement of recognition performance is to find more discriminative representations of

modulated signals for neural network. The constellation diagrams and spectrogram images are used as the input features of convolutional neural networks (CNN) in [13, 14].

Since the superposition of signals in the power domain will make the constellation change obviously, the joint constellation density diagrams of NOMA signals are selected as the shallow representation, and then a deep residual network [15] for feature learning and classification is designed for realizing the detection of modulation mode of far UT's signal in NOMA system. The main contributions of this paper include:

- Introducing DL algorithm to detect modulation mode of NOMA signals.
- Designing preprocessing algorithm to improve the classification performance, which includes wavelet denoising and density extraction.
- Analyzing three factors that affect the detection performance of NOMA modulation signal by numerical experiments.

Notations: The notation meaning of this paper is shown in **Table 1**.

Table 1. Table of Notation

Notation	Meaning
$ A $	Euclidean norm of a scalar A
$E[A]$	The expectation value of a random event A
A^*	The conjugate of complex number A
$I(A)$	The imaginary part of complex number A
$P(A)$	The real part of complex number A
$\lceil A \rceil$	The ceiling of number A
$\lfloor A \rfloor$	The floor of float number A
$len(A)$	Calculate length of vector A
e	Euler's number

2. System Model

A downlink NOMA scenario is considered in this paper, where a BS communicates with N UTs. N_c UTs share the same sub-channel after user grouping, which can be called co-scheduled users. According the rules of superposition coding [16], the NOMA signal is generated by the superposition of N_c UTs signals with specified power ratios, which is can be expressed as:

$$s = \sum_{i=1}^{N_c} \sqrt{\alpha_i P_i} x_i, \quad N_c \leq N \quad (1)$$

where P_i is total transmitting power and x_i represents the transmitted signal of the i -th user UT_i . α_i represents the power ratio assigned to UT_i and satisfied $\sum_i \alpha_i = 1$.

The power allocation algorithms of NOMA system can be divided into optimal and suboptimal allocation algorithms [17]. Among them, since the optimal power distribution algorithms, such as the iterative water-filling algorithm, often has too much computation,

fractional transmit power allocation algorithms is adopted in this system model. The transmission power of UT_i is expressed as:

$$\alpha(i) = \frac{1}{\sum_{j \in S} (g(j)/n(j))^{-\alpha_{fpc}}} \left(\frac{g(i)}{n(i)} \right)^{\alpha_{fpc}} \quad (2)$$

where $g(j)$ represents channel gain vector. $n(j)$ is the power of noise and interference signals. S is a set of UTs. α_{fpc} denotes the decay factor, which satisfies $0 < \alpha_{fpc} < 1$. As α_{fpc} increases, more power is allocated to the far UT since its channel condition is poor.

For the convenience of analyzing, the scenario considered is that there are two co-scheduled UTs. The two-user NOMA system is shown in Fig. 1 and it can be developed into a system model including more UTs.

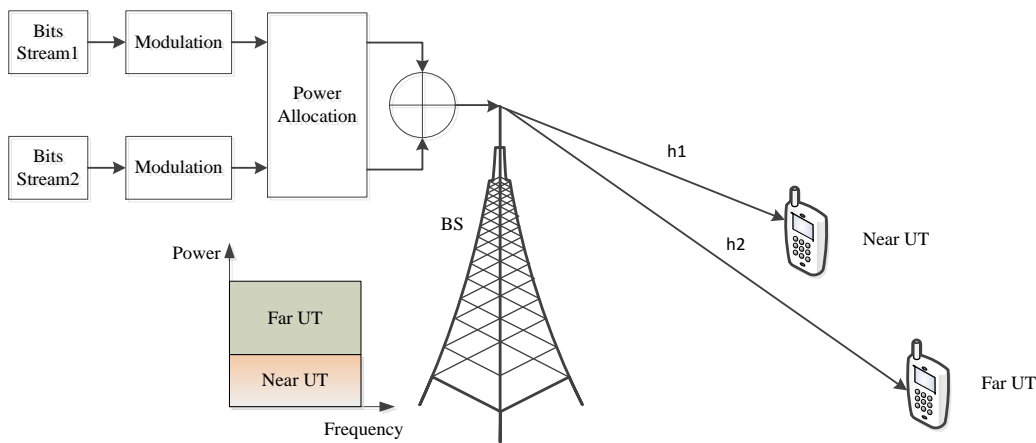


Fig. 1. A simple downlink two-user NOMA

The received signal of near UT can be written as:

$$s(k) = h(k)(\sqrt{\alpha_1 P_1} x_1(k) + \sqrt{\alpha_2 P_1} x_2(k)) + w(k), \quad k = 1, 2, \dots, K \quad (3)$$

where K represents the length of each transmitted signal. $x_1(k)$ and $x_2(k)$ is modulated signal sent to near user and far user respectively. α_1 and α_2 denotes power ratios, which satisfies $\alpha_1 + \alpha_2 = 1$ and $\alpha_2 > \alpha_1$. $h(k)$ represents channel fading, which is Rayleigh distribution with $E\{|h(k)|^2\} = \sigma_1^2$, and $w(k)$ is white Gaussian noise with zero mean and variance N_0 .

In the decoding process of superimposed coding scheme, the received signal of far UT is decoded directly because $x_1(k)$ are regarded as noise. The received signal of near UT first decodes $x_2(k)$, then reconstructs $x_2(k)$ and cancellation it from the received signal, and then decodes $x_1(k)$. For the above decoding scheme, it is necessary to require the near UTs to know

the modulation mode of the far UTs, so that the interference of the far UTs can be removed validly. Therefore, a DL algorithm is introduced to realize the modulation blind detection for NOMA system in this paper.

3. Proposed Algorithm

3.1 The joint constellation density diagrams

The constellation of NOMA signal is the superposition of the multi-user's constellation, which is called the joint constellation diagram. When the component signals of NOMA signal are modulated in different ways or different power allocation ratio, the distribution of its joint constellation will change. So the joint constellation can be used as a feature of NOMA modulation detection, which can be shown in Fig. 2. Fig. 2(a) is the joint constellation is obtained by superposition coding of 16-QAM modulated signals and $\pi/2$ -BPSK modulated signals without considering power allocation, where modulation scheme of near UT is set to 16-QAM. If we carry power allocation in NOMA system, the distribution of the joint constellation will change. Fig. 2(b) is the joint constellation when $\beta=0.5$ and signal to noise ratio (SNR) difference between near UT and far UT is 6dB.

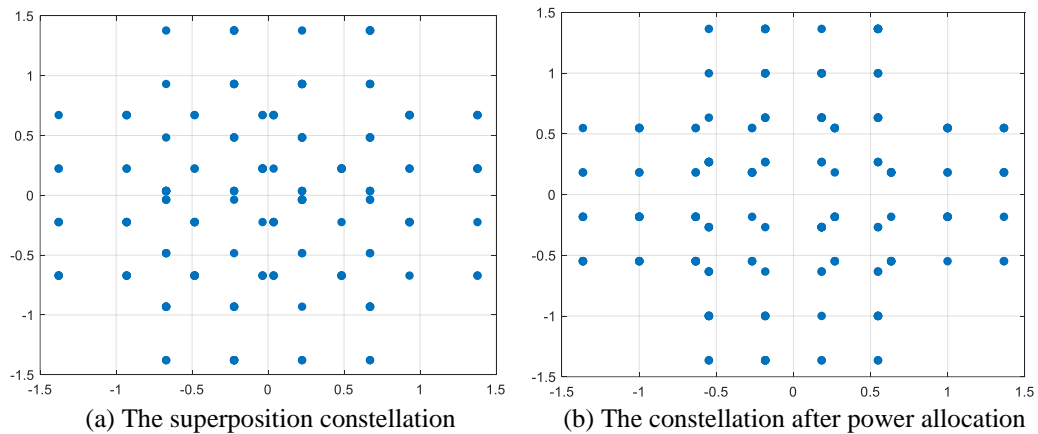


Fig. 2. The joint constellation diagrams

When the SNR is not ideal, the distribution pattern of the constellations will be easily lost, so the quality of the joint constellation diagrams need be improved by denoising first. The traditional denoising method is to filter out the frequency part of the noise by passing the band-pass filter. When the frequency band of the noise is very wide, it is difficult to separate the noise from the effective signal. The multi-resolution of wavelet transform (WT) can make the active components of non-stationary signal and noise show different characteristics respectively [18]. The amplitude of wavelet coefficients generated by the WT of the effective signal is larger than the wavelet coefficients of the noise. The WT of signal $x(t)$ can be written as:

$$WT_x(a,b) = \frac{1}{\sqrt{a}} \int x(t) \psi^* \left(\frac{t-b}{a} \right) dt \quad (4)$$

where b is time shifting and a represent scale factor. $\psi(t)$ is denoted basic wavelet.

The NOMA signal was separated into real part and imaginary part and computed the wavelet decomposition respectively. Then soft thresholding is applied to the detail wavelet coefficients and wavelet reconstruction is realized according to the original approximation coefficients and the modified detail coefficients. Lastly, the denoising results of the real and imaginary parts are combined to achieve the overall denoising of NOMA signal. The detailed process of wavelet denoising for NOMA signal is shown in **Fig. 3**.

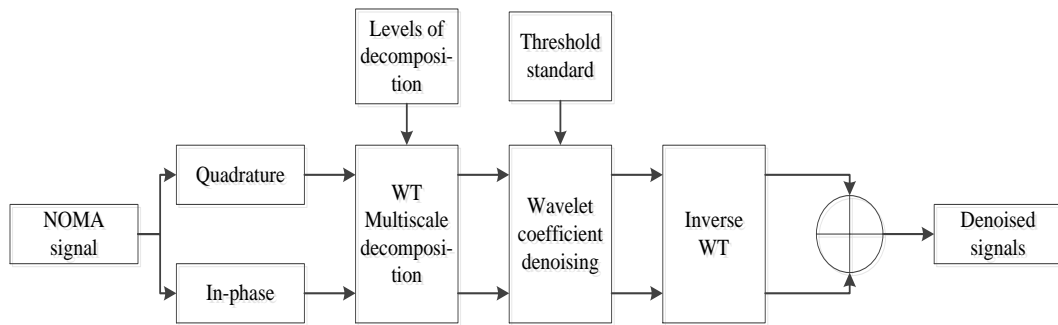


Fig. 3. The process of wavelet denoising for NOMA signal

With the increase of noise components in communication system, the number of wavelet levels need be adaptively increased. In order to reduce the computational complexity, the parameters of wavelet transform are fixed in our work. Simulation experiment is design to test the denoising performance on NOMA signal by adjusting the parameters of wavelet transform, and then select the appropriate wavelet parameters and detailed simulation parameters of wavelet denoising is shown in **Table 2**.

Table 2. Simulation parameters of preprocessing

Parameter	Value	Parameter	value
Near UT modulation mode	16-QAM	Basic wavelet	sym8
Far UT modulation mode	$\pi/2$ -BPSK	Thresholding rule	heursure
Near UT SNR	16 dB	Thresholding type	soft thresholding
Far UT SNR	10 dB	The level of the WT	2

Fig. 4 shows the joint constellation diagram after denoising. The noise is suppressed and effective signal is retained by wavelet denoising for NOMA signal, so the joint constellation diagram has more obvious characteristics and tends to an ideal distribution, which is more easily classified by neural networks.

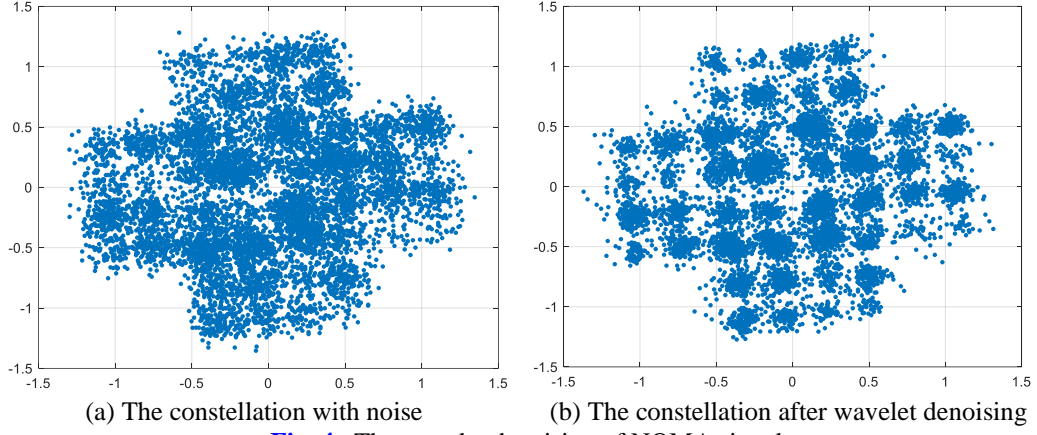


Fig. 4. The wavelet denoising of NOMA signal

Considering there be multiple signal sample points within the range of one pixel, so not every point in a constellation has its value for signal classification. After density extraction of constellation, the pixel value of constellation points can be used as a distinguishing feature. The constellation density is calculated by counting the number of sample points in the fixed region. Then normalizes the constellation density and converts it into the pixel value of the region. Finally, a grayscale image is generated. The density extraction process can be described by Algorithm 1 and the joint constellation density diagram is shown in Fig. 5.

Algorithm 1. The joint constellation density diagram

Input: The NOMA signal $s(k)$ after wavelet denoising

Output: The joint constellation density diagram matrix G with size of $L \times L$

1: Into two orthogonal groups:

$$x = I(s(k)), y = R(s(k))$$

2: Finding the minimum of x and y

$$\min_x = \min(x), \min_y = \min(y)$$

3: Matrix coordinate transformation

$$x = \lceil x - \min(x) \rceil, y = \lceil y - \min(y) \rceil$$

4: Generating the joint constellation matrix C

for i in range($\text{len}(x)$) do

for j in range($\text{len}(y)$) do

$$C(x, y) = 1$$

end for

end for

5: Determining statistical area

$$W = \lfloor x / L \rfloor, H = \lfloor y / L \rfloor$$

6: Count the number of constellation points in an area and generating the statistical matrix CT

7: Normalization to grayscale matrix G

$$G(i, j) = \frac{CT(i, j) - \min(CT)}{\max(CT) - \min(CT)}$$

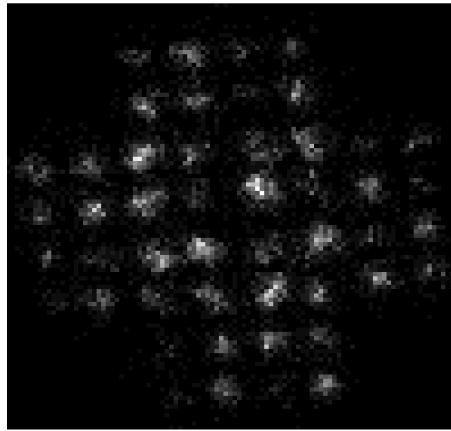


Fig. 5. The grayscale joint constellation density diagram

The joint constellation density diagram obtained by preprocessing algorithm not only strengthened the differentiation for different NOMA signal constellations, but also adjusted the size of the matrix to make it more suitable as an input matrix for neural network.

3.2 Deep Residual Network

When the neural network have reached optimal network depth, and then still increase the number of network layers, the classification accuracy of neural network will often become worse, which is called network degradation. Reference [15] designed a residual learning framework to ease the training of networks. With the introduction of residual learning, neural network is easier for the redundancy layer to realize identity mapping, so as to solve the problem of network degradation.

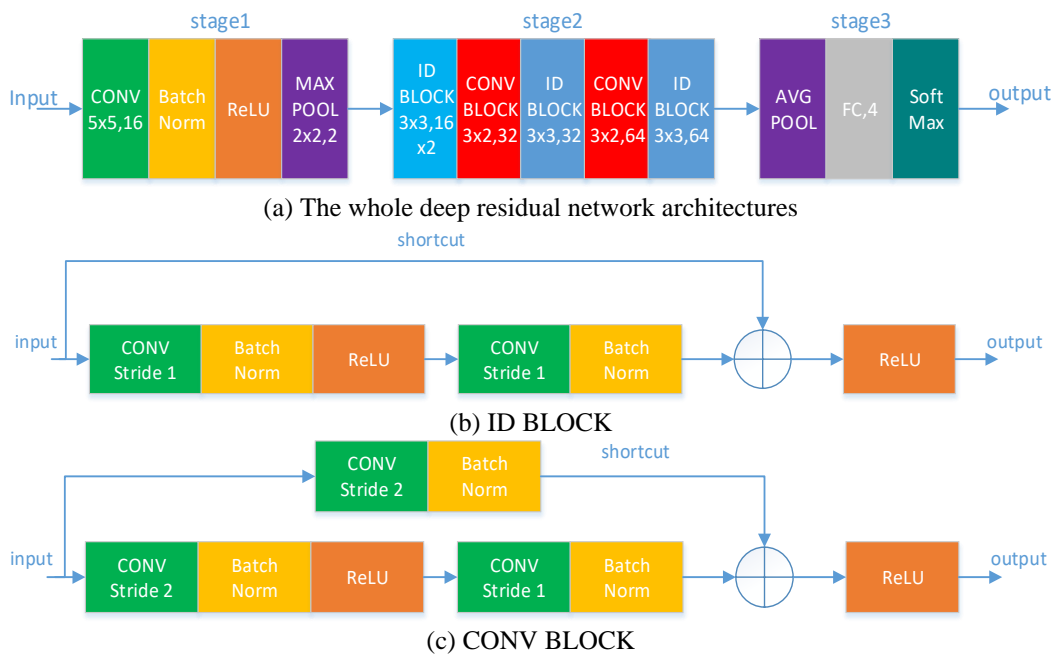


Fig. 6. The deep residual network for modulation detection

In this paper, deep residual network is designed to detect the modulation mode of NOMA signal. The input of the network is the joint constellation density diagrams with size of 100×100 matrix. The whole network architectures can be divided into three stages, which is shown as **Fig. 6(a)**.

In the first stage, the network extracts the characteristics of the bottom layer through a baseline convolution layer. Batch Normalization layer is added after convolution, which pulls the data distribution back to the standard normal distribution with zero mean and variance one, so that the input value of the nonlinear transformation ReLU function falls into the region that is more sensitive to the input, which can avoid the gradient disappearance problem. Then feature maps are down-sampled by max-pooling.

In the second stage, the deep features are excavated through 6 residual blocks. There are two types of residual blocks in **Fig. 6(b)** and **Fig. 6(c)**. One is the identity block in the case of consistent input and output, which is denoted by ID BLOCK. The other is the convolutional block in the case of inconsistent input and output, which is denoted by CONV BLOCK. It includes the convolution operation in the shortcut, and the output matrix is half the size of the input matrix for each CONV BLOCK.

In the last stage, the feature matrixes are down-sampled by average-pooling first. After flattening, it passes through a fully connected layer, which contains four output neural nodes. The last layer calculates the output probability for each neural node by softmax activation function, which can be written as (5).

$$S_i = \frac{e^{a_i}}{\sum_j e^{a_j}}$$

where T are all categories of NOMA modulation scheme. a^i represents the i -th output of the network. The cross entropy loss of the predicted modulation scheme and the expected modulation scheme, which can be expressed as (6), is used as the loss function to drive the training of the whole network.

$$Loss = -\sum_i^T y_i \ln S_i \quad (5)$$

where y_i represents the expected modulation scheme, which have been encoded one-hot label.

4. Simulation and Comparison

In the simulation, each user can choose the modulation schemes supported by the current 5G standard, which are $\pi/2$ -BPSK, QPSK, 16-QAM and 64-QAM. With the same SNR and modulation scheme, there are 1000 NOMA signal samples, and the dividing ratio of training set, validation set and test set is 6 to 2 to 2 for the whole dataset. The detailed simulated parameters of NOMA system are shown in **Table 3**. In the training processing of residual network, the stochastic gradient descent with momentum (SGDM) is used as the optimization method of network. The initial learning rate is 0.01 and learning rate schedule is piecewise constant decay. The iterations per epoch are 800 and max epoch is set 10. The batch size is set to 64 when data is batched into the network. The elapsed training time is 8 minutes and 31

seconds on single GTX 1050 Ti GPU.

Table 3. The simulated parameters of NOMA system

Parameter	Value	Parameter	Value
The length of symbol	1024	Transmitted power	1W
Symbol rate	1KBaud	Channel	AWGN
Carrier frequency	2GHz	Fast fading	Rayleigh
Sampling rate	3.2MHz	The range of SNR(dB)	-10:2:20
Modulation scheme	PSK/QAM	Decay factor	0.2/0.5/0.8

Since the distribution of the joint constellation diagrams are mainly affected by the types of modulation mode of NOMA signal, the number of UTs and power allocation between MU, numerical simulation is designed to verify the influence of these three factors for the modulation detection accuracy of NOMA in this paper.

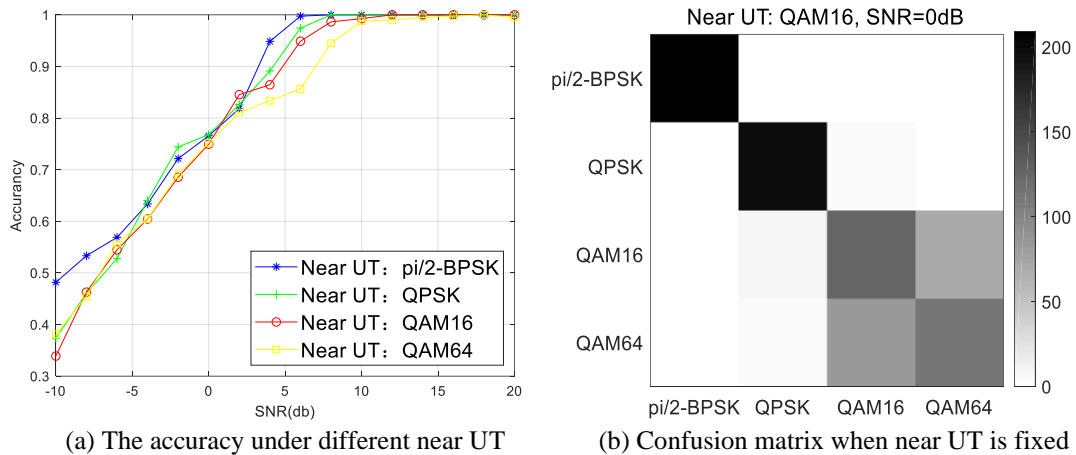


Fig. 7. The detection accuracy for different modulation scheme of UTs

In the case of fixed power allocation ratio, **Fig. 7** represents the detection accuracy under different modulation scheme of near UT. When the SNR is above 2dB, **Fig. 7(a)** shows the modulation recognition accuracy will decrease with the increase of the near UT's modulation order. **Fig. 7(b)** shows that the high-order modulation of far UT will misclassify each other when the 16-QAM is applied to near UT and SNR is set to 0dB. If the 16-QAM or 64-QAM is applied to far UT, the transmitted symbol will be a 256-QAM-liked or 1024-QAM-liked symbol respectively [19], which will be more difficult to classify them correctly for neural network. It is worth mentioning in **Fig. 7** that although the constellation of $\pi/2$ -BPSK is also of fourth order modulation, its distribution is more characteristic than QPSK. However, the joint constellation diagrams have been polluted by noise to a large extent under 2dB, and the effect of the wavelet denoising with fixed parameters is not obvious. So the recognition rate is roughly the same when the high-order modulation is used.

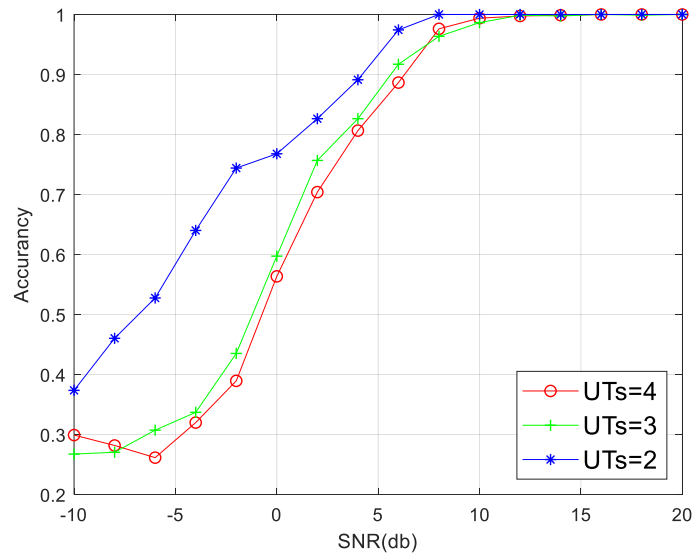


Fig. 8. The detection accuracy for different numbers of UTs

In the simulation of **Fig. 8**, the number of far UT is set to 1, and the number of near UTs is set to 1, 2 and 3, respectively. Different near UTs get different power ratios due to different locations and are modulated in the same QPSK scheme. The modulation mode of Far UT can be $\pi/2$ -BPSK, QPSK, 16-QAM and 64-QAM. The simulation result shows the detection accuracy will decrease with the increase of the number of users, because the joint constellation becomes more complicated.

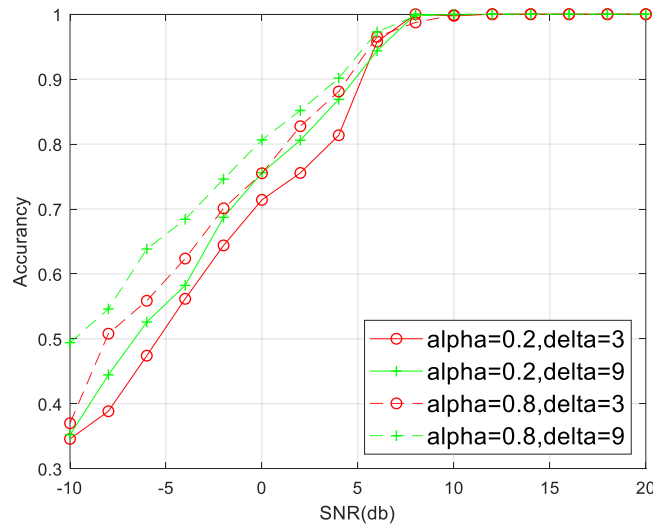


Fig. 9. In the case of the same near UT, the detection accuracy with different power allocation ratio

When power allocation is carried out in NOMA system, the allocation ratio is positively correlated with the SNR difference between near UT and far UT, which is denoted by 'delta' in **Fig. 9**, and the decay factor in fractional power allocation algorithm, which is denoted by 'alpha' in **Fig. 9**. When the 'alpha' or the 'delta' is large, the detection accuracy of modulation mode will be improved. This is because the larger the 'alpha' or 'delta' made the far UT get

more large power factor, then the overall distribution of the joint constellation would be biased towards the constellation of far UT, as shown in **Fig. 2(a)** and **Fig. 2(b)**, which will be easy to implement the correct classification by deep residual network.

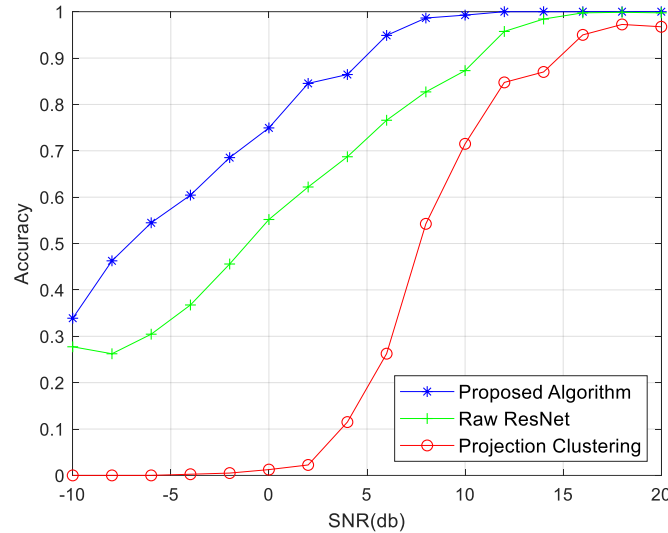


Fig. 10. The detection accuracy in different modulation detection algorithms

The proposed algorithm is compared with the traditional modulation recognition algorithm based on projection subtractive clustering of constellations, which is denoted by Projection Clustering in **Fig. 10**, and using the joint constellations without preprocessing as the input image of the network, which is denoted by Raw ResNet in **Fig. 10**. The projection clustering algorithm needs to calculate the number of clustering centers first. With the increase of constellation points, the complexity of the clustering algorithm in the traversal process will be higher. In addition, the robustness against noise of cluster algorithm is poor, whether it is subtractive clustering or K-means clustering. When the SNR is not ideal, the representation ability of the joint constellation without wavelet denoising is obviously reduced. Consequently, the modulation detection algorithm based on the joint constellation density diagrams and deep residual network is superior to the other two methods in NOMA systems.

5. Conclusion

Wireless communication channel has been considered by many researchers is the largest black box in the physical layer. NOMA signals often have a certain extent of distortion and loss at the receiving terminal. The application of machine learning algorithm to help the communication system processes the unknown information over the air, which can achieve greater performance than traditional methods. In this paper, The NOMA signal modulation detection algorithm based on the joint constellation density diagrams and deep residual network is proposed, which will reduce the signaling overhead in the communication system and improve the demodulation efficiency of SIC. However, for the existing high-order modulation mode in 5G, such as 256-QAM, its constellation will be more complex, and the classification difficulty will be significantly increased, which is where further research is needed.

References

- [1] Z. Ding, X. Lei, G. K. Karagiannidis, R. Schober, J. Yuan, and V. K. Bhargava, "A Survey on Non-Orthogonal Multiple Access for 5G Networks: Research Challenges and Future Trends," *IEEE Journal on Selected Areas in Communications*, vol. 35, no. 10, pp. 2181-2195, Oct. 2017. [Article \(CrossRef Link\)](#)
- [2] S. M. R. Islam, N. Avazov, O. A. Dobre, and K. Kwak, "Power-Domain Non-Orthogonal Multiple Access (NOMA) in 5G Systems: Potentials and Challenges," *IEEE Communications Surveys & Tutorials*, vol. 19, no. 2, pp. 721-742, Sep. 2017. [Article \(CrossRef Link\)](#)
- [3] B. Ling, C. Dong, J. Dai, and J. Lin, "Multiple Decision Aided Successive Interference Cancellation Receiver for NOMA Systems," *IEEE Wireless Communications Letters*, vol. 6, no. 4, pp. 498-501, Aug. 2017. [Article \(CrossRef Link\)](#)
- [4] F. Haitao, W. Qun, and S. Rong, "Modulation Classification Based on Cyclic Spectral Features for Co-Channel Time-Frequency Overlapped Two-Signal," in *Proc. of Pacific-Asia Conference on Circuits, Communications and Systems*, pp. 31-34, May 2009. [Article \(CrossRef Link\)](#)
- [5] M. Choi, D. Yoon, and J. Kim, "Blind Signal Classification for Non-Orthogonal Multiple Access in Vehicular Networks," *IEEE Transactions on Vehicular Technology*, vol. 68, no. 10, pp. 9722-9734, Oct. 2019. [Article \(CrossRef Link\)](#)
- [6] W. Wei and J. M. Mendel, "Maximum-likelihood classification for digital amplitude-phase modulations," *IEEE Transactions on Communications*, vol. 48, no. 2, pp. 189-193, Feb. 2000. [Article \(CrossRef Link\)](#)
- [7] N. Zhang, K. Cheng, and G. Kang, "A Machine-Learning-Based Blind Detection on Interference Modulation Order in NOMA Systems," *IEEE Communications Letters*, vol. 22, no. 12, pp. 2463-2466, Dec. 2018. [Article \(CrossRef Link\)](#)
- [8] X. You, C. Zhang, X. Tan, S. Shi, and H. Wu, "AI for 5G: research directions and paradigms," *Science China (Information Sciences)*, vol. 62, Oct. 2018. [Article \(CrossRef Link\)](#)
- [9] K. B. Letaief, W. Chen, Y. Shi, J. Zhang, and Y. A. Zhang, "The Roadmap to 6G: AI Empowered Wireless Networks," *IEEE Communications Magazine*, vol. 57, no. 8, pp. 84-90, Aug. 2019. [Article \(CrossRef Link\)](#)
- [10] G. Gui, H. Huang, Y. Song, and H. Sari, "Deep Learning for an Effective Nonorthogonal Multiple Access Scheme," *IEEE Transactions on Vehicular Technology*, vol. 67, no. 9, pp. 8440-8450, Sep. 2018. [Article \(CrossRef Link\)](#)
- [11] J. M. Kang, I. M. Kim, and C. J. Chun, "Deep Learning-Based MIMO-NOMA With Imperfect SIC Decoding," *IEEE Systems Journal*, vol. 14, no. 3, pp. 3414-3417, Sep. 2020. [Article \(CrossRef Link\)](#)
- [12] N. E. West and T. O'Shea, "Deep architectures for modulation recognition," in *Proc. of IEEE International Symposium on Dynamic Spectrum Access Networks*, pp. 1-6, May 2017. [Article \(CrossRef Link\)](#)
- [13] S. Peng, H. Jiang, H. Wang, H. Alwageed, Y. Zhou, M. M. Sebdani, and Y. D. Yao, "Modulation Classification Based on Signal Constellation Diagrams and Deep Learning," *IEEE Transactions on Neural Networks and Learning Systems*, vol. 30, no. 3, pp. 718-727, Mar. 2019. [Article \(CrossRef Link\)](#)
- [14] Y. Zeng, M. Zhang, F. Han, Y. Gong, and J. Zhang, "Spectrum Analysis and Convolutional Neural Network for Automatic Modulation Recognition," *IEEE Wireless Communications Letters*, vol. 8, no. 3, pp. 929-932, June 2019. [Article \(CrossRef Link\)](#)
- [15] K. He, X. Zhang, S. Ren, and J. Sun, "Deep residual learning for image recognition," in *Proc. of IEEE Conference on Computer Vision and Pattern Recognition*, pp. 770-778, June 27-30, 2016. [Article \(CrossRef Link\)](#)
- [16] S. Vanka, S. Srinivasa, Z. Gong, P. Vizi, K. Stamatiou, and M. Haenggi, "Superposition Coding Strategies: Design and Experimental Evaluation," *IEEE Transactions on Wireless Communications*, vol. 11, no. 7, pp. 2628-2639, July 2012. [Article \(CrossRef Link\)](#)

- [17] N. Otao, Y. Kishiyama, and K. Higuchi, "Performance of non-orthogonal access with SIC in cellular downlink using proportional fair-based resource allocation," *IEICE Transactions on Communications*, vol. 98, no. 2, pp. 344-351, Feb. 2015. [Article \(CrossRef Link\)](#)
- [18] X. Gu, "Research on modulation recognition algorithm of digital communication signal based on wavelet denoising," *Applied Mechanics & Materials*, pp. 459-467, Oct. 2014. [Article \(CrossRef Link\)](#)
- [19] Q. He, Y. Hu, and A. Schmeink, "Closed-Form Symbol Error Rate Expressions for Non-Orthogonal Multiple Access Systems," *IEEE Transactions on Vehicular Technology*, vol. 68, no. 7, pp. 6775-6789, July 2019. [Article \(CrossRef Link\)](#)



Wenwu Xie was born in Jingzhou, Hubei, China in 1979. He received the B.S., M.S. and Ph.D. degrees in communication engineering from the Huazhong Normal University in 2004, 2007 and 2017. From 2007 to 2009, he was a communication algorithm engineer in spreadtrum communication CO. LTD. His research interests include communication algorithm, such as channel estimation, equalizer and encoding/decoding and so on. And he holds two patents. Since 2017, he was a lecture in Hunan Institute of Science and Technology (HNIST).



Jian Xiao was born in Hengyang, Hunan, China in 1994. He received the B.S. degree in electronic information engineering from the HNIST in 2019. Since 2019, he was a Master student in HNIST. His major research interests include reconfigurable intelligent surface and machine learning.



Ji Wang received the B.S. degree from the School of Electronic Information and Communications, Huazhong University of Science and Technology, China, in 2008, and the Ph.D. degree from the School of Information and Communications Engineering, Beijing University of Posts and Telecommunications, China, in 2013. He held postdoctoral positions with the School of Electronic Information and Communications, Huazhong University of Science and Technology, and the Department of Electrical Engineering, Columbia University, USA. His research interests include space information networks and B5G wireless communications.



Jinxia Yang was born in Shaoyang, Hunan, China in 1998. She received the B.S. degree in communication engineering from the HNIST in 2019, she was a Master student in HNIST. Her major research interests include physical layer secrecy and reconfigurable intelligent surface.



Xin Peng received the B.S. degree in communication engineering from Hunan University, Changsha, China, in 2003. Then he received his M.S. degree and Ph.D. degree in computer science from Hunan University, Changsha, China, in 2008 and 2011, respectively. He was a visiting researcher at Auburn University, USA, in 2014. His main research interests include Internet of Things, CPS and Cloud Computing.



Chao Yu was born in Yueyang, Hunan, China in 1986. He received the B.S. degree and M.S. degree in communication engineering from the Guilin Electronic Technology University in 2009 and 2012. He received the Ph.D. degrees at Hoseo University in Korea. His research interests include UAV and reconfigurable intelligent surface.



Peng Zhu was born in Yueyang, Hunan, China in 1990. He received the Ph.D. degrees in space physics from the Wuhan University. His major research interests in signal processing and communication techniques.